Journal of Plant Growth Regulation (2023) 42:5558–5573
https://doi.org/10.1007/s00344-023-10936-x

Nitric Oxide and Glutathione Act Synergistically to Improve PSII Activity and PSI Electron Transfer Under Chilling Stress in Cucumber Leaves

Zhifeng Yang[1,2] · Xiaoyu Wang[1,2] · Jinxia Cui[1,2] · Huiying Liu[1,2] · Huimei Cui[1,2] · Pei Wu[1,2]

Received: 9 December 2021 / Accepted: 11 November 2022 / Published online: 27 February 2023

Abstract

The present study investigated the interaction between reduced glutathione (GSH) and nitric oxide (NO) in enhancing the cold tolerance of cucumber seedlings. In this study, cold-sensitive 'Jinyan No. 4' cucumber seedlings were used as test materials. Four different treatments, including CK: distilled water (control), DS: distilled water + 200 μmol L^{-1} sodium nitroprusside (SNP), BS:1 mmol L^{-1} buthionine sulfoximine (BSO) + SNP, and SG: 200 μmol L^{-1} SNP + 5 mmol L^{-1} GSH were used to pretreat cucumber leaves. Pretreated cucumber seedling leaves were used for the analysis after 24 h and 48 h under low temperature (10 °C day/6 °C night). The results showed that compared with the control, DS and SG treatments could maintain lower K-step (48 h) and L-step (48 h) and higher P-step on the OJIP transient curve. The application of DS and SG also increased the values of maximal redox capacity of photosystem I (PSI) ($\Delta I/I_o$), the primary photochemical efficiency (F_v/F_o), the maximum photochemical efficiency (F_v/F_m), the photosynthetic performance index (PI_{ABS}) (48 h), quantum yield for reducing the terminal electron acceptor on the acceptor side of PS I (φ_{Ro}), the phenomenological energy fluxes per excited cross section (ABS/CS_m, TR_o/CS_m, and ET_o/CS_m), and the density of per reaction center (RC/CS_m), while decreasing some others like the relative variable fluorescence at J-step (V_J) (48 h), the quantum ratio of thermal dissipation (F_o/F_m), the dissipated energy flux per CS (DI_o/CS_m), and the specific energy fluxes per reaction center (DI_o/RC), with the highest effect being observed in SG treatment. Furthermore, DS and SG treatments were observed a low level of hydrogen peroxide and superoxide, the enhancement of proline content, and some enzyme activities (AsA-GSH cycle), and the combined effect of SNP and GSH is more prominent than the single effect of SNP. In addition, BSO (GSH synthase inhibitor) can abolish or reverse the effect of SNP. Our results suggest that GSH may act downstream of NO to improve cold tolerance of cucumber seedlings under low-temperature stress, and more interestingly, NO and GSH play a synergistic role in mitigating the adverse effects of low-temperature stress.

Keywords Cucumber seedling · Low temperature · Antioxidant enzymes · Prompt fluorescence · JIP-test

Abbreviations

NO	Nitric oxide
SNP	Sodium nitroprusside
BSO	Buthionine sulfoximine

Handling Editor: M.Iqbal R. Khan.

Zhifeng Yang and Xiaoyu Wang have contributed equally to this study.

✉ Jinxia Cui
jinxiacui77@163.com

Zhifeng Yang
zhifengyangmr@163.com

Xiaoyu Wang
wangxy9992021@163.com

Huiying Liu
hyliuok@aliyun.com

Huimei Cui
chmagr@shzu.edu.cn

Pei Wu
1448928895@qq.com

[1] Department of Horticulture, Agricultural College, Shihezi University, Shihezi 832003, Xinjiang, China

[2] Key Laboratory of Special Fruits and Vegetables Cultivation Physiology and Germplasm Resources Utilization of Xinjiang Production and Construction Crops, Shihezi 832003, Xinjiang, China

GSH	Reduced glutathione
Pro	Proline
GR	Glutathione reductase
MDHAR	Monodehydroascorbate reductase
DHAR	Dehydroascorbate reductase
GPX	Glutathione peroxidase
GST	Glutathione-*S*-transferase
PSII	Photosystem II
PSI	Photosystem I
ROS	Reactive oxygen species
AsA-GSH	Ascorbate–glutathione cycle
γ-ECS	γ-Glutamylcysteine synthetase
GSNO	*S*-Nitrosoglutathione
$O_2^{-\bullet}$	Superoxide
H_2O_2	Hydrogen peroxide
NBT	Nitro-blue tetrazolium
DAB	3,3′-Diaminobenzidine
EL	Electrolyte leakage
Q_A	Primary quinone electron acceptor of PSII
Q_B	Secondary quinone electron acceptor of PSII
PQ	Plastoquinone
RC	The reaction center
ABS	Absorption energy flux
TR	The capture of excitation energy

Introduction

Abiotic stresses affect every crop cultivated around the globe at various scales (Zandalinas et al. 2018). Among the different abiotic stresses, cold severely limits crop productivity (Ding et al. 2019). Low temperature (0 ~ 10 °C) induces overproduction of reactive oxygen species (ROS) leading to oxidative damage through peroxidation of membrane lipids, leakage of solutes from cells, and chlorophyll loss. Excessive production of ROS inhibits the repair of photodamaged photosystem II (PSII) at low temperatures (Asada 2006; Miller et al. 2007). Cucumber (*Cucumis sativus* L.) is a tropical-origin vegetable crop, which is sensitive to low temperatures (Cabrera et al. 1992). In particular, cucumber seedlings are susceptible to low-temperature injury during off-season cultivation, such as during winter and early spring cultivation in the unheated solar greenhouse (Zhou et al. 2007). Therefore, it is necessary to study the low-temperature tolerance mechanism of cucumber.

Nitric oxide (NO) is an essential endogenous signaling molecule mediating a diverse array of plant biological processes including responses to various stresses. Numerous reports have demonstrated that appropriate concentrations of NO act as a cue that mediates plant growth and enhances tolerance to stresses such as low temperature, high temperature, drought, salt stress, and heavy metal pollution (Sun et al. 2021). The application of NO increases iron utilization in plants, thereby promoting chlorophyll biosynthesis (Tewari et al. 2021). The 80% of the iron in plant leaves is present in chloroplasts, and this iron is bound in thylakoid membrane proteins, which help maintain the structural and functional integrity of thylakoid membranes (Adamski et al. 2011). Therefore, the accumulation of iron is conducive to the efficiency of photosynthesis (Nam et al. 2021). Besides, NO application could upregulate the leaf gas exchange parameters G_s, C_i, E, and P_N, as well as chlorophyll fluorescence parameters such as F_v/F_m, ϕ_{PSII}, q_P, and photosynthetic electron transport rate to improve the overall photosynthetic efficiency when plants were exposed to abiotic stresses (Khoshbakht et al. 2018). Ascorbate–glutathione cycle (AsA-GSH) is an essential antioxidant system for eliminating ROS in plants. Monodehydroascorbate reductase (MDHAR), dehydroascorbate reductase (DHAR), glutathione reductase (GR), glutathione peroxidase (GPX), and glutathione-*S*-transferase (GST) are important enzymatic components in the AsA-GSH cycle (Gupta et al. 2015). Exogenous sodium nitroprusside (SNP) improves tolerance to abiotic stresses in plants by modulating the AsA-GSH cycle (Hu et al. 2019). GSH is a tripeptide compound containing thiol that can eliminate oxidative stress induced by abiotic stresses (Hasanuzzaman et al. 2017). GSH can not only directly detoxify ROS through the catalysis of GPX to protect the structure and function of cysteine sulfhydryl, but also participate in the scavenging of ROS in the AsA-GSH system. In addition to the detoxification of electrophilic compounds, GSH acts as a signal in plants (Hasanuzzaman et al. 2017; Waszczak et al. 2018; Ma et al. 2020). Similar to the effect of NO, the application of GSH can increase gas exchange parameters and chlorophyll fluorescence parameters to enhance photosynthetic reactions under adversity (Zhou et al. 2018). Under Cd stress, *Arabidopsis thaliana* plants treated with $_L$-buthionine sulfoximine (BSO, an inhibitor of γ-glutamylcysteine synthetase, γ-ECS) showed increased phytotoxicity due to decreased GSH content (Wojcik and Tukiendorf 2011; Zandalinas et al. 2018; Zhou et al. 2018).

The collaboration of NO and GSH is evidenced by *S*-nitrosoglutathione (GSNO). In plants, GSNO is mobile and stabilize NO storage, and it could be decomposed by the enzyme GSNO reductase (GSNOR) to GSSG, in turn, which is reduced to GSH by GR-dependent post-translational modification (Lindermayr 2017). Notably, GSNO exerts a positive influence on plant resistance. Under heat stress, the application of GSNO to rice leaves improved P_N, rubisco activation status, F_v/F_m, and Φ_{PSII}, which was beneficial to the recovery of photosynthesis and the elimination of hydrogen peroxide (H_2O_2) accumulation (Song et al. 2013). The drought resistance of *Lolium perenne* was improved, and ROS homeostasis was maintained through exogenous GSNO (Rigui et al. 2019). Similarly, exogenous GSNO could improve sugarcane growth and photosynthesis under

the water deficit condition (Silveira et al. 2016). Moreover, NO and GSNO have also been shown to have separable and overlapping functions in the development of plant immunity, possibly due to their redox-modulate the activity of different target proteins (Yun et al. 2016).

The above-mentioned reports show that NO, GSH, and its possible theoretical product GSNO have a positive impact on plant resistance. For instance, the co-treatment of the SNP and GSH remarkably inhibited the absorption and transport of copper by rice seedlings (Mostofa et al. 2015). External application of SNP (a NO donor) significantly increased the level of endogenous NO, regulated the redox level of GSH, affected photosynthesis capacity, and enhanced cold resistance (Wang et al. 2017; Zhang et al. 2019). In recent years, many studies have found synergistic effects of co-application with different bioactive substances and GSH in alleviating the stress of adversity. Zeng et al. (2021) showed that the combination of GSH and citric acid could enhance lead stress tolerance in castorbean by increasing antioxidant enzyme activity and decreasing MDA and H_2O_2 levels. Under chromium stress, the combined treatment of GSH and putrescine significantly increased the bioaccumulation of endogenous GSH and promoted recovery in yield traits in canola stems compared to the single application of GSH or putrescine (Jahan et al. 2021). Goodarzi et al. (2020) found that the combined application of GSH and melatonin improved the ability of safflower to tolerate large amounts of zinc by increasing AsA-GSH cyclase activity and AsA/DHA and GSH/GSSG ratios. Dawood et al. (2020) revealed that the combined application of GSH and selenium alleviated wheat salt stress by significantly enhancing the content of photosynthetic pigments, carbohydrates, flavonoids, phenolics and growth hormones. The synergistic effect of GSH and selenium in alleviating salt stress was also confirmed in sweet pepper (Elkhatib et al. 2021). The combination of GSH and moringa oleifera leaf extract significantly alleviated salt stress-induced imbalance in ion homeostasis and osmotic stress in wheat (Rehman et al. 2021).

NO and GSH are well-known regulators of stress tolerance, but their interactions in regulating low-temperature tolerance still require further investigation. Therefore, in this experiment, cucumber 'Jinyan No.4' was used as material to study the effects of SNP combined with BSO and GSH on the Pro content and AsA-GSH cycle-related enzyme activities under chilling stress. The Kautsky effect-based chlorophyll fluorescence technique, a convenient and non-invasive method for assessing photosynthetic activity, reveals the difference in cucumber dark and cold response between different treatments. Furthermore, the collective effects of NO and GSH on mitigating cold-induced damage in cucumber were evaluated by PSII activity and its electron transfer in PSI, and responses of the antioxidant defense system.

Materials and Methods

Plant Material

The experiment was conducted at the Experimental Station of the Agricultural College of Shihezi University, Xinjiang, in China (45°19' N, 74°56′ E) from May to August 2019. Cucumber (*Cucumis sativus* L.) 'Jinyan No. 4' was used for the study. Healthy and uniform cucumber seeds were selected and disinfected by soaking in 55 °C hot water for 15 min, then the seeds were further soaked in distilled water for 6 h at room temperature. After completing the above steps, the cucumber seeds were incubated on moist filter paper and transferred to RXZ-300c intelligent artificial incubator (Ningbo Jiangnan Instrument Factory) in dark at 28 °C for 18 h. The germinating seeds with the same sprout length were selected and sown in 72-hole plugs. When the cotyledons were flattened, the seedlings were moved into a bowl (120 mm × 110 mm) containing a mixture of the nutrient substrate (peat: vermiculite: perlite = 1:1:1, the peat pore size is 10–30 mm), one seedling per container. After 4 days of adaptation, 60 mL of Hoagland's nutrient solution was irrigated every four days. The seedlings were used for the experiment when they reached two true leaves.

Experimental Procedures

Cucumber seedlings were sprayed with four experimental treatments as shown in Fig. 1 (cucumber seedlings were sprayed with the corresponding solutions uniformly on the abaxial and the adaxial side of the two true leaves and the shoot apex). After the samples were last sprayed with treatment for 2 h, the seedlings were transferred to a PERCIVAL E-36 L plant incubator (Percival, USA). The conditions of the artificial climate incubator were set to 30 °C/14 h during the day, 15 °C/10 h at night, the light intensity of 300 μmol·m^{-2}·s^{-1} and the relative humidity of 50%. The seedlings were pre-cultured for one day in a plant incubator, and on the second day at 10:00 am, the seedlings were exposed to low temperatures. The conditions of low temperature were 10 ± 1 °C/14 h during the day, 6 ± 1 °C/10 h at night, the light intensity of 100 μmol•m^{-2}•s^{-1}, and the relative humidity of 75%. The second leaves from the bottom were harvested accordingly for different analyses at 24 and 48 h after low temperature (Fig. 1a). This trial used a single-factor completely randomized design.

a

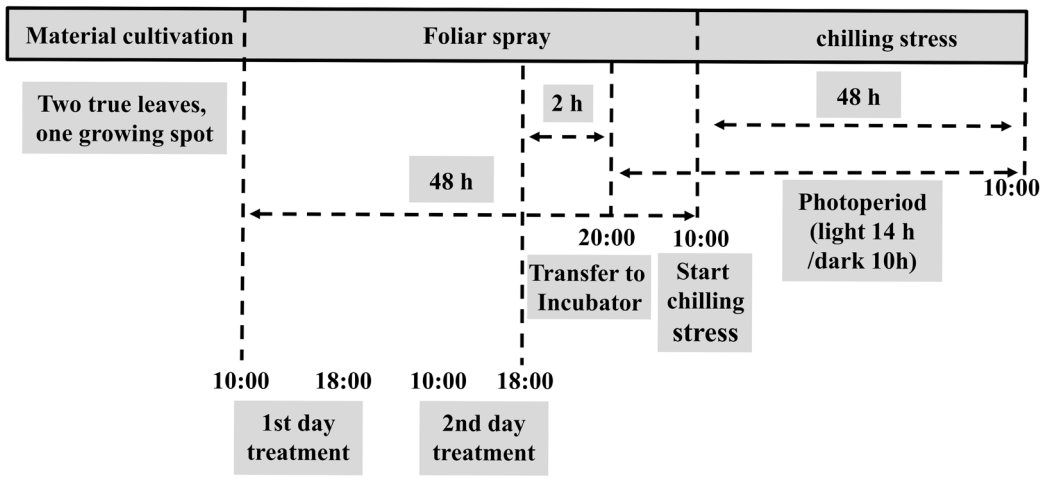

b

Description of different treatments

Spraying Time	CK (Control)	DS	BS	SG
10:00	Distilled water	Distilled water	BSO	SNP
18:00	Distilled water	SNP	SNP	GSH

Note: SNP, 200 μmol·L^{-1} sodium nitroprusside (NO donor); BSO, 1 mmol·L^{-1} buthionine sulfoximine, (GSH synthetase inhibitor); GSH, 5 mmol·L^{-1} reduced glutathione

Fig.1 A scheme of the treatments used to study the effect under low temperature in cucumbers (**a**). Description of different treatments (**b**)

Determination of Pro Content and Electrolyte Leakage (EL) in the Leaves

The Pro content of cucumber leaves was determined according to the method of Li (2000). Electrolyte leakage (EL) was measured referring to the method of Rai et al. (2018). Cucumber leaf disks (0.1 g) were incubated in 10 mL of deionized water at room temperature (EL1) for 12 h and others at 100 °C (EL2) for 30 min. The EL was measured by using a conductivity meter (DSJ-1 Digital Conductivity Meter, Shanghai). The membrane stability index was estimated as per the following equation. EL(%) = (EL1/EL2) × 100.

Determination of the AsA-GSH Cycle-Related Enzyme Activities in Leaves

GR (EC 1.6.4.2), MDHAR (EC 1.6.5.4), DHAR (EC 1.8.5.1), and GPX (EC 1.11.1.9) activities were determined according to the method of Zhou et al. (2018). GST (EC 2.5.1.18) activity was determined according to the method of Booth et al. (1961). The protein content was determined according to the method of Li (2000).

Histochemical Staining

Histochemical staining of superoxide ($O_2^{-\bullet}$) and hydrogen peroxide (H_2O_2) was conducted according to the method described by Thordal-Christensen (1997). Distilled water was used to fully rinse the 2nd true leaf of the cucumber seedling. Leaf disks (1 cm in diameter), respectively, were stained in a reaction solution containing 10 mL of 0.1% nitro-blue tetrazolium (NBT) (25 mmol·L^{-1} HEPES, pH 7.8) and 1 mg•mL^{-1} diaminobenzidine (DAB) (1 mg•mL^{-1} DAB, 50 mM Tris–HCl, pH 3.8) for 8 h at 28 °C. Then, the staining solution was removed and the leaf disks were placed in 95% ethanol and boiled for 10 min for decolorization observation. The blue color indicates the degree of $O_2^{-\bullet}$ accumulation and the brown color indicates the degree of H_2O_2 accumulation.

Measurement of Fast Chlorophyll Fluorescence Curve and 820 nm Light Absorption Curve in Cucumber Leaves

The prompt chlorophyll fluorescence curve and 820 nm light absorption curve in cucumber leaves were determined by referring to the method of Strasser et al. (2010). After being treated with dark adaptation for 1 h, the second true leaves of cucumber seedlings were used to measure the prompt chlorophyll fluorescence curve (O-K-J-I-P curve) and the 820-nm transmission change by Multi-Function Plant Efficiency Analyzer (M-PEA). The LED with a light intensity of 3000 μmol•m^{-2}·s^{-1} was used as the light source. Fluorescence signal started from 0.01 ms and ended at 3 s and recorded 138 data with 0.01 ms (0.01 ~ 0.3 ms), 0.1 ms (0.3 ~ 3 ms), 1 ms (3 ~ 30 ms), 10 ms (30 ~ 300 ms), and 100 ms (300 ~ 3000 ms) interval recording fluorescence signal. There were three replicates of each treatment, and the average value was taken as the measured value of the instantaneous fluorescence induction kinetic curve of the treated leaves. The relative value of the difference between the maximum value of 820 nm light absorption (I_o) and the minimum value (I_m), i.e., $\Delta I/I_o = (I_o - I_m)/I_o$, was used as an indicator of PSII activity. The O-K-J-I-P curve was analyzed with the OJIP-test (Mishra 2018). In the analysis, F_o equaled the fluorescence level at 50 μs (O-step), F_K equaled fluorescence level at 300 μs (K-step), the F_J equaled fluorescence level at 2 ms (J-step), F_I equaled fluorescence level at 30 ms (I-step), and F_m was the maximum fluorescence (P-step). We have calculated the following parameters (Table 1).

Statistical Analysis

Microsoft Excel 2016 was used for data analysis. Data were analyzed by one-way analysis of variance (ANOVA) and Duncan multiple comparisons using SPSS version 23.0. Data were expressed as the mean ± standard deviation (SD) of three replicates, and Origin 2018 was used for preparing graphs. The figure of correlation analysis was prepared by R language software with the corroplot package (version 3.50).

Results

Staining of $O_2^{-\bullet}$ and H_2O_2 in Leaves

In this study, we pretreated cucumber leaves with BSO, a key enzyme inhibitor for GSH synthesis. To determine whether GSH is involved in NO accumulation and the low-temperature tolerance of cucumber seedlings, we investigated the $O_2^{-\bullet}$ and H_2O_2 accumulation in cucumber leaves by histochemical staining with NBT and DAB, respectively (Fig. 2). Both $O_2^{-\bullet}$ (blue spots) and H_2O_2 (brown spots) were observed to be distributed throughout the leaves in CK treatment after 24 h and 48 h of low temperature. Both DS and SG treatments reduced the low temperature-induced $O_2^{-\bullet}$ and H_2O_2 in cucumber leaves compared to CK. Notably, BS treatment reversed the above effect, observing more $O_2^{-\bullet}$ (blue spots) with H_2O_2 (brown spots) than in DS treatment.

Pro Content and EL

We pretreated cucumber leaves with BSO, a key enzyme inhibitor for GSH synthesis, to investigate the role of GSH in NO accumulation and low-temperature tolerance. EL reflects the degree of damage to the cell membrane. The cold tolerance response of the plants was reflected by measuring the Pro content. Exposure of cucumber seedlings to low temperatures led to an increase in EL and an increase in Pro content (Fig. 3). During the whole low-temperature period, DS treatment significantly increased Pro content and significantly decreased EL compared to CK. Specifically, after 24 and 48 h of low temperature, DS treatment significantly increased Pro by 140.10% and 87.50%, respectively (Fig. 3a), and significantly decreased EL by 54.72% and 39.41%, respectively (Fig. 3b), compared to CK. Conversely, compared to DS, BS significantly inhibited the accumulation of SNP-induced Pro and the decrease of SNP-induced EL. In addition, compared to DS, the SG treatment significantly increased Pro by 27.67% and decreased EL by 25.06% at low temperature for 48 h.

AsA-GSH Cycle-Related Enzyme Activities

The GR, MDHAR, DHAR, GPX, and GST are important components of the AsA-GSH cycle, and thus their activities are closely related to the clearance of ROS. Compared with CK, exogenous NO positively influenced the ability of ROS scavenging in cucumber leaves under low-temperature stress. After plants were exposed to low temperature for 24 and 48 h, DS treatment significantly increased GR activity (35.35% and 33.17%), MDHAR activity (30.70% and 29.57%), DHAR activity (16.28% and 52.75%), GPX activity (83.24% and 64.78%), and GST activity (8.85% and 15.33%), respectively, compared with CK. In contrast, BS significantly diminished the SNP-induced increase in GR, MDHAR, DHAR, GPX, and GST activities compared with DS during the whole low-temperature period. At 24 h of low-temperature treatment, the scavenging of ROS in SG plants (except GPX) was more effective than that of the DS treatment. Compared with DS, SG treatment significantly increased GR, MDHAR, GPX, and GST activities by 11.12%, 11.69%, 5.98%, and 38.81%, respectively, at a low temperature of 48 h (Fig. 4).

Table 1 Formulae and terms used in the kinetics of prompt fluorescence and modulated light reflection at 820 nm

Formulae and terms	Illustrations
Information selected for the fast OJIP fluorescence induction (data necessary for the calculation of the so-called JIP parameters)	
$F_o = F_{50\mu s}$	Minimal recorded fluorescence intensity, the $F_{50\mu s}$ data point to be used as the F_o parameter value
F_m	Maximal fluorescence intensity (when all RCs are closed)
F_k	Fluorescence intensity at the k-step (at 300 µs)
F_J	Fluorescence intensity at the J-step (at 2 ms)
F_I	Fluorescence intensity at the I-step (at 30 ms)
$F_v = F_m - F_o$	Maximum variable Chl fluorescence
$V_t = (F_t - F_o)/(F_m - F_o)$	Relatively variable fluorescence (F_t refers to fluorescence at any moment)
t_{Fm}	Time to reach a maximal fluorescence intensity F_m
$W_k = (F_k - F_o)/(F_J - F_o)$	Relative variable fluorescence at the K-step (at 300 µs)
$V_J \equiv (F_J - F_o)/(F_m - F_o)$	Relative variable fluorescence at the J-step (at 2 ms)
$V_I \equiv (F_J - F_o)/(F_m - F_o)$	Relative variable fluorescence at the I-step (at 30 ms)
$\Delta V_t = V_{t\ (treatment)} - V_{t\ (CK)}$	ΔV_t is the normalized fluorescence difference between other treatments and the control curve. The difference between O-J, J-I, and I-P curves and CK is represented by ΔV_{O-J}, ΔV_{J-I} and ΔV_{I-P}, respectively.
$M_o \equiv 4(F_{300\mu s} - F_o)/(F_m - F_o)$	The approximate initial slope of the fluorescence transient, which is the maximum rate of Q_A being reduced
$dV/dt_0 = (F_{150\mu s} - F_o)/(F_m - F_o)$	The slope at the origin of the relative variable fluorescence is a measure of the rate of primary photochemistry $((dQ_A^-/Q_{A\ (total)})/dt_0)$
$S_m \equiv (Area)/(F_m - F_o)$	Normalized area (proportional to the number of reduction and oxidation of one Q_A molecule or the number of electron carriers per electron transport chain)
S_m/t_{Fm}	The average redox state of Q_A in the time span from F_o to t_{Fm} (the average fraction of open reaction centers during the time needed to complete their closure)
N	The number of times Q_A has been reduced in the time span from 0 to F_m (a measure of the energy needed to close all reaction centers)
Yields or flux ratios	
$\varphi_{Po} \equiv TR_o/ABS = [1 - (F_o/F_m)] = F_v/F_m$	The maximum quantum yield of primary PSII photochemistry
$\psi_{Eo} \equiv ET_o/TR_o = 1 - V_J$	Efficiency/probability that an electron moves further than Q_A^-
$\varphi_{Eo} \equiv ET_o/ABS = [1 - (F_o/F_m)] \cdot \psi_o$	Quantum yields for electron transport
$\delta_{Ro} = (1 - V_I)/(1 - V_J)$	Efficiency/probability with which an electron from the intersystem electron carriers is transferred to reduce end electron acceptors at the PSI acceptor site (RE)
$\varphi_{Ro} = [1 - (F_o/F_m)] \cdot (1 - V_I)$	Quantum yield for reduction of end electron acceptors at the PSI acceptor site (RE)
$\gamma_{RC} = Chl_{RC}/Chl_{total} = RC/(ABS + RC)$	The probability that a PSII Chl molecule functions as RC
$RC/ABS = \gamma_{RC}/(1 - \gamma_{RC}) = \varphi_{Po}(V_J/M_o) = (ABS/RC)^{-1}$	The probability that a PSII Chl molecule functions as RC
$\psi_o \equiv ET_o/TR_o = (1 - V_J)$	The probability (at $t = 0$) that a trapped exciton moves an electron into the electron transport chain beyond Q_A^-
Specific energy fluxes [per Q_A-reducing PSII reaction center (RC)]	
$ABS/RC = M_o \cdot (1/V_J) \cdot (1/\varphi_{Po})$	Absorption flux per RC
$DI_o/RC = (ABS/RC) - (TR_o/RC)$	Dissipated energy flux per RC (at $t = 0$)
$TR_o/RC = M_o \cdot (1/V_J)$	Trapped energy flux per RC (at $t = 0$)
$ET_o/RC = M_o \cdot (1/V_J) \cdot \psi_o$	Electron transport flux per RC (at $t = 0$)
$RE_o/RC = M_o \cdot (1/V_J) \cdot (1 - V_I)$	Electron flux reducing end electron acceptors at the PSI acceptor site, per RC
Phenomenological energy fluxes [per exciting cross section (CS), When $t = t_{Fm}$, CS_o was replaced by CS_m, $ABS/CS_m \approx F_m$.]	
$ABS/CS_o \approx F_o$	Absorption flux per CS (at $t = 0$)
$DI_o/CS_o = (ABS/CS_o) - (TR_o/CS_o)$	Dissipated energy flux per CS (at $t = 0$)
$TR_o/CS_o = \varphi_{Po} \cdot (ABS/CS_o)$	Trapped energy flux per CS (at $t = 0$)

Table 1 (continued)

Formulae and terms	Illustrations
$ET_o/CS_o = \varphi_{Eo} \cdot (ABS/CS_o)$	Electron transport flux per CS (at $t = 0$)
RE_o/CS_o	Electron flux reducing end electron acceptors at the PSI acceptor site, per CS
Performance indexes	
$PI_{ABS} \equiv [\gamma_{RC}/(1-\gamma_{RC})] \cdot [\varphi_{Po}/(1-\varphi_{Po})] \cdot [\psi_o/(1-\psi_o)]$	Performance index on absorption basis
Information selected from the modulated light reflection at 820 nm (Alamri et al. 2020)	
$\triangle I/I_o = (I_o - I_m)/I_o$	The measure of maximum PSI activity (I_o is the maximum value of 820 nm light absorption and I_m is the minimum value of 820 nm light absorption)

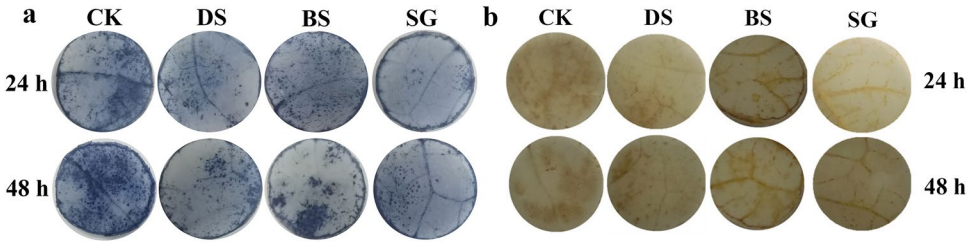

Fig. 2 Effect of exogenous SNP and GSH on the staining of $O_2^{-\bullet}$ (**a**) and H_2O_2 (**b**) in leaves of cucumber seedlings under low temperature

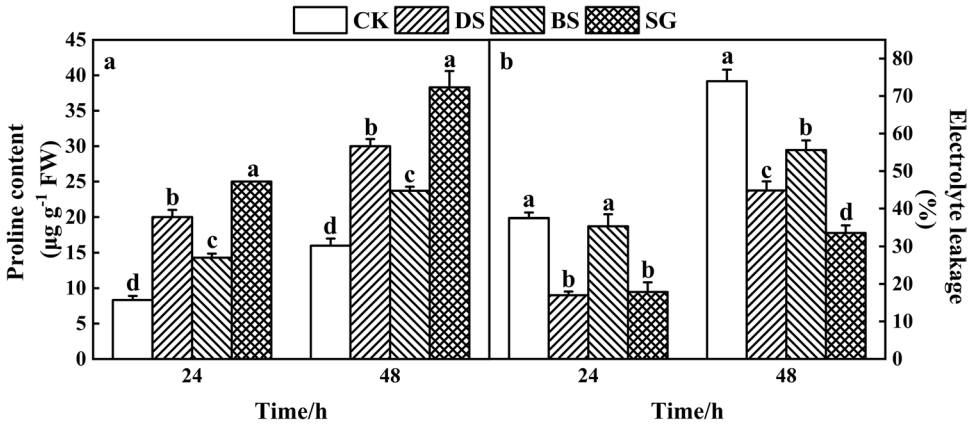

Fig. 3 Proline content (**a**) and Electrolyte leakage (**b**) in cucumber leaves under low-temperature stress (day (10 ± 1) °C/14 h, night (6 ± 1) °C/10 h) following different treatments. The value is the mean ± SD ($n = 3$). Different letters in each panel indicate statistically significant differences ($P < 0.05$)

Prompt Fluorescence Parameters

It was apparent from Figs. 5a and b that the F_o of each treatment was different with the prolongation of low-temperature stress. It indicated that the background fluorescence of the excited pigment started to show differences after complete dark adaptation. The difference in background fluorescence was affected by multiple factors (quantity, activity), which indicated that the treatment group had a potential impact on photosynthesis. In comparison with CK, the initial fluorescence of each treatment was not much different. The fluorescence intensity of DS and SG treatments gradually increased, and it was more prominent when fluorescence intensity reached point P (the P point of SG is the largest) (Fig. 5a). It was shown that at the short-term low temperature, DS and SG treatments alleviated the decline of the fluorescence yield of cucumber leaves. When the stress duration was extended to 48 h, the initial fluorescence of DS and SG was significantly lower than that of CK and BS, and the value at the point of P was the largest (Fig. 5b), indicating that at the prolonged low temperature, SG treatment more effectively alleviated the fluorescence downtrend. V_t (Fig. 5c) and ΔV_t (Fig. 5d) ($\Delta V_t < 0$) of DS and SG treatments in the J-step were lower at low temperature for 48 h, indicating that the closing of the active reaction center (P_{680}) by DS and SG treatments was less at this time. The electron transfer activity from Q_A to Q_B was higher than CK, and DS and SG treatments did not cause PSII reaction center receptor site Q_A^- accumulation. It could rapidly promote the continuous reduction of the plastoquinone (PQ) pool, increase the electron-accepting capacity of the PQ pool, and facilitate the electron transfer capacity from PSII receptor

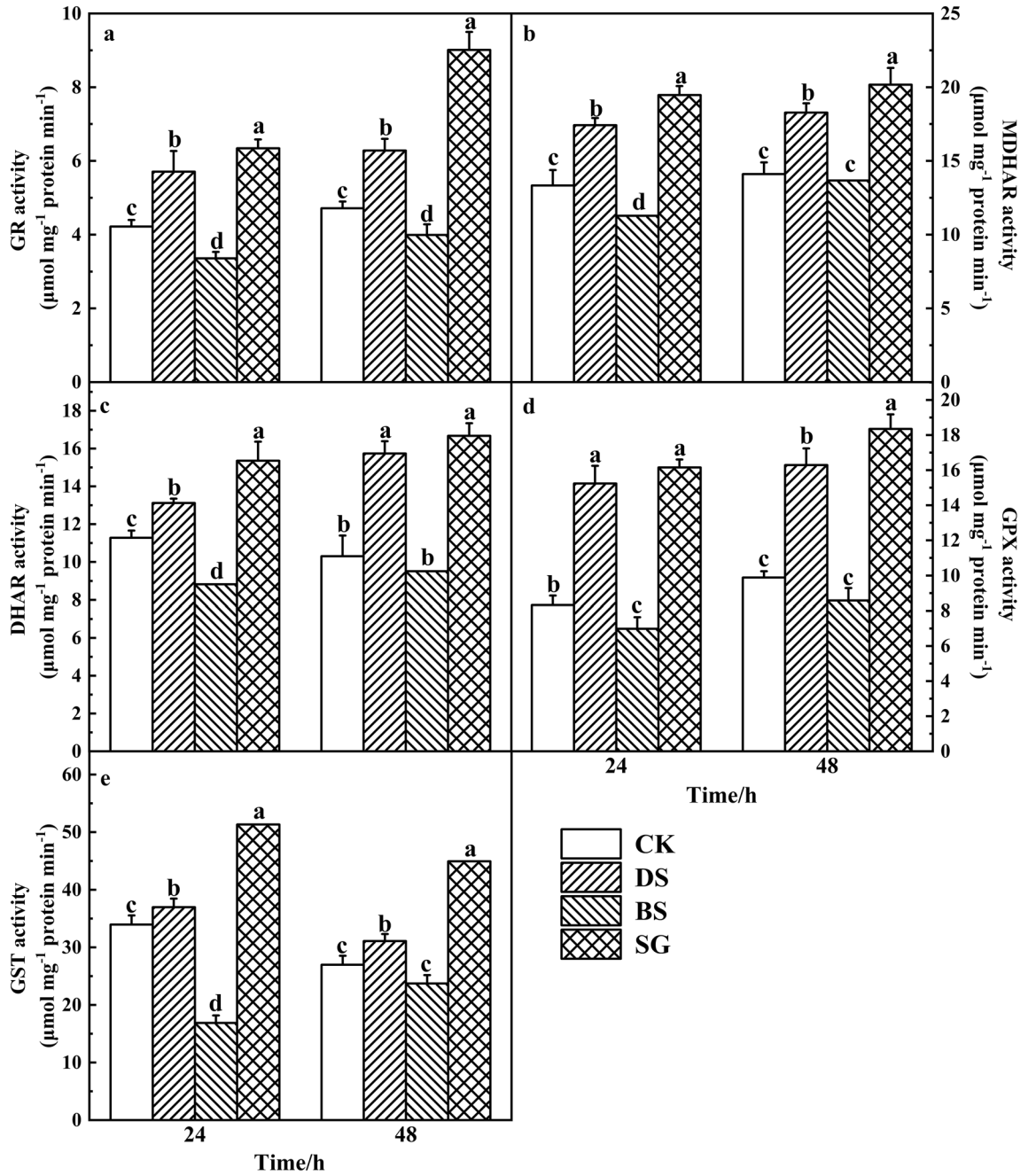

Fig. 4 The GR (**a**), MDHAR (**b**), DHAR (**c**), GPX (**d**), and GST (**e**) activity in cucumber leaves after low-temperature stress (day (10 ± 1) °C/14 h, night (6 ± 1) °C/10 h). The value is the mean ± SD ($n = 3$). Different letters in each panel indicate statistically significant differences ($P < 0.05$)

site Q_A to Q_B. The lower ΔV_t (Fig. 5d) in the I-step for DS and SG treatments during the low temperature for 48 h demonstrates that the electron transport activity from Q_B to PSI was higher than that in CK in all cases.

Transient Fluorescence Induction Kinetic Characteristics (JIP-test)

In contrast to CK, the DS and SG treatments were able to significantly increase the quantum efficiency per unit area exposed to light (ABS/CS_m, TR_o/CS_m, ET_o/CS_m, RE_o/CS_m, RE_o/CS_o) and decrease the activity parameters (DI_o/CS_o, DI_o/RC) associated with thermal dissipation at a shorter

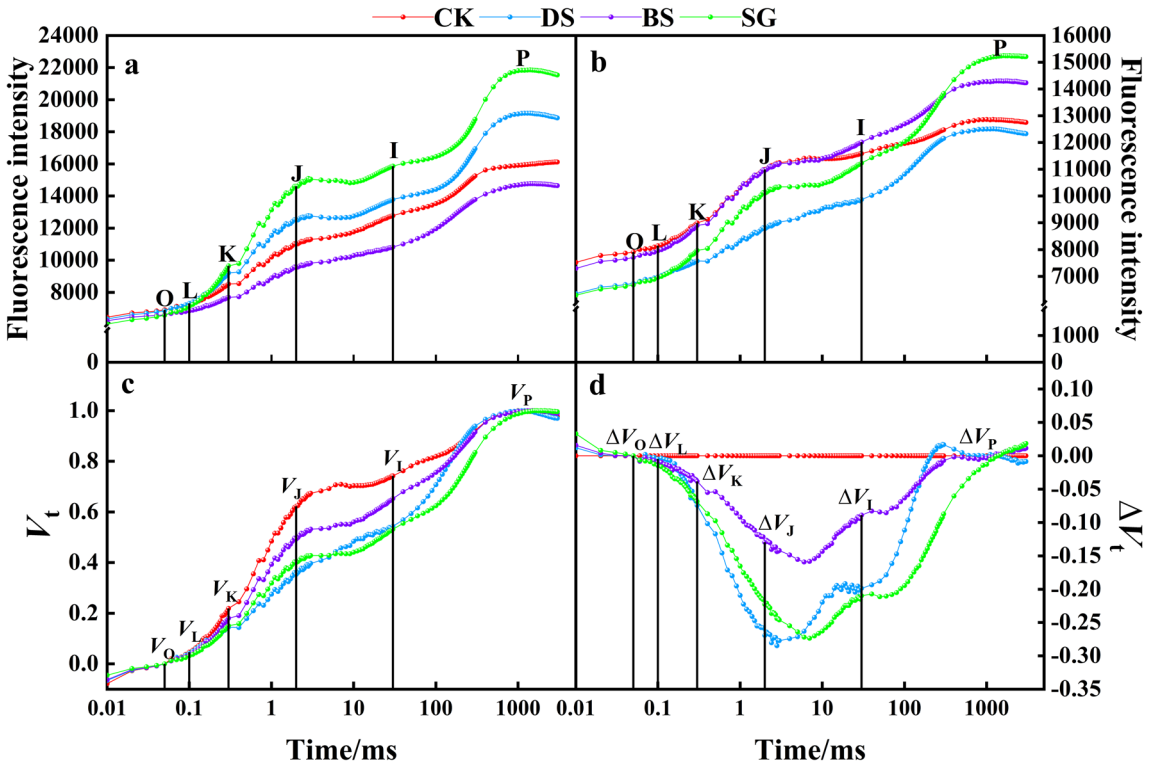

Fig. 5 The fast chlorophyll fluorescence curve of cucumber seedling leaves under low-temperature stress after different treatments. **a** Fluorescence intensity under low-temperature stress for 24 h, **b**, **c**, **d** Fluorescence intensity, Vt, and ΔV_t under low-temperature stress for 48 h. **a** and **b** The change of chlorophyll *a* fluorescence OJIP. **c** A standardized OJIP curve, plotted with relative variable fluorescence (V_t), $V_t=(F_t–F_o)/(F_m–F_o)$. **d** The change of the differential curve, plotted with the normalized fluorescence difference (ΔV_t) between treatment and control data, $\Delta V_t = V_{t\ (treatment)}\text{-}V_{t\ (CK)}$

time (24 h) at low temperature (Fig. 6a). In comparison with CK, DS and SG treatments dramatically increased the JIP-test parameters S_m, S_m/t_{Fm}, δ_{Ro}, φ_{Ro}, and F_v/F_o at low temperature for 24 h. This indicated that DS and SG treatments could boost the light energy of electron absorption and electron transfer to PSI terminals by increasing not only the capacity of PSII receptor site pools but also the conversion efficiency of Q_A oxidation and re-reduction. The results also showed that DS and SG treatments could accelerate the photochemical rate by not only improving the capacity of the PSII receptor site pool, but also the efficiency of electron absorption and electron transfer to the PSI terminal (Fig. 6c). In addition to the above results, the increase in photochemical rate by DS and SG treatments was further verified by the significant increase in t_{Fm} with the extension of low-temperature duration to 48 h compared to CK (Fig. 6d).

As shown in Fig. 7, compared with CK, treatment with DS, BS and SG followed by exposure of cucumber plants to low temperature for 48 h resulted in elevated PI_{ABS}, $(\gamma_{RC}/(1\text{-}\gamma_{RC})$, $(\varphi_{Po}/(1\text{-}\varphi_{Po})$, $\psi_o/(1\text{-}\psi_o)$ and F_v/F_m. DS, BS, and SG treatments improved PI_{ABS} by 271.99%, 163.59%, and 570.03%, respectively, and DS, BS and SG treatments improved F_v/F_m by 31.34%, 19.29%, and 44.31%, respectively, compared with CK, revealing that inhibition of GSH biosynthesis greatly attenuated the positive effect of NO on these photosynthetic parameters. It is noteworthy that PI_{ABS} was more sensitive to low-temperature stress than F_v/F_m, implying that PI_{ABS} was more suitable as a parameter for measuring the adverse effect of low-temperature stress on photosynthetic parameters. The value of PI_{ABS} for SG treatment was much greater than the other treatments, indicating that SG was the most effective in restoring photosynthetic capacity. Meanwhile, compared with CK, SG treatment promoted $(\varphi_{Po}/(1\text{-}\varphi_{Po})$ and $\psi_o/(1\text{-}\psi_o)$ by 102.55% and 130.62%, respectively, and the promotion effect was greater than the other treatments. It means that SG treatment maintained high photosynthetic capacity, which was mainly achieved by increasing the light energy absorption efficiency and electron acceptor acceptance efficiency.

Low temperature-induced photoinhibition can be assessed by measuring the activity of the photosynthetic machinery. To determine the effect of each treatment on PSI, we analyzed the $\Delta I/I_o$ of each treatment under low-temperature conditions. The values of $\Delta I/I_o$ under different treatments showed an overall decreasing trend with the extension of low-temperature time (Fig. 8). The DS treatment

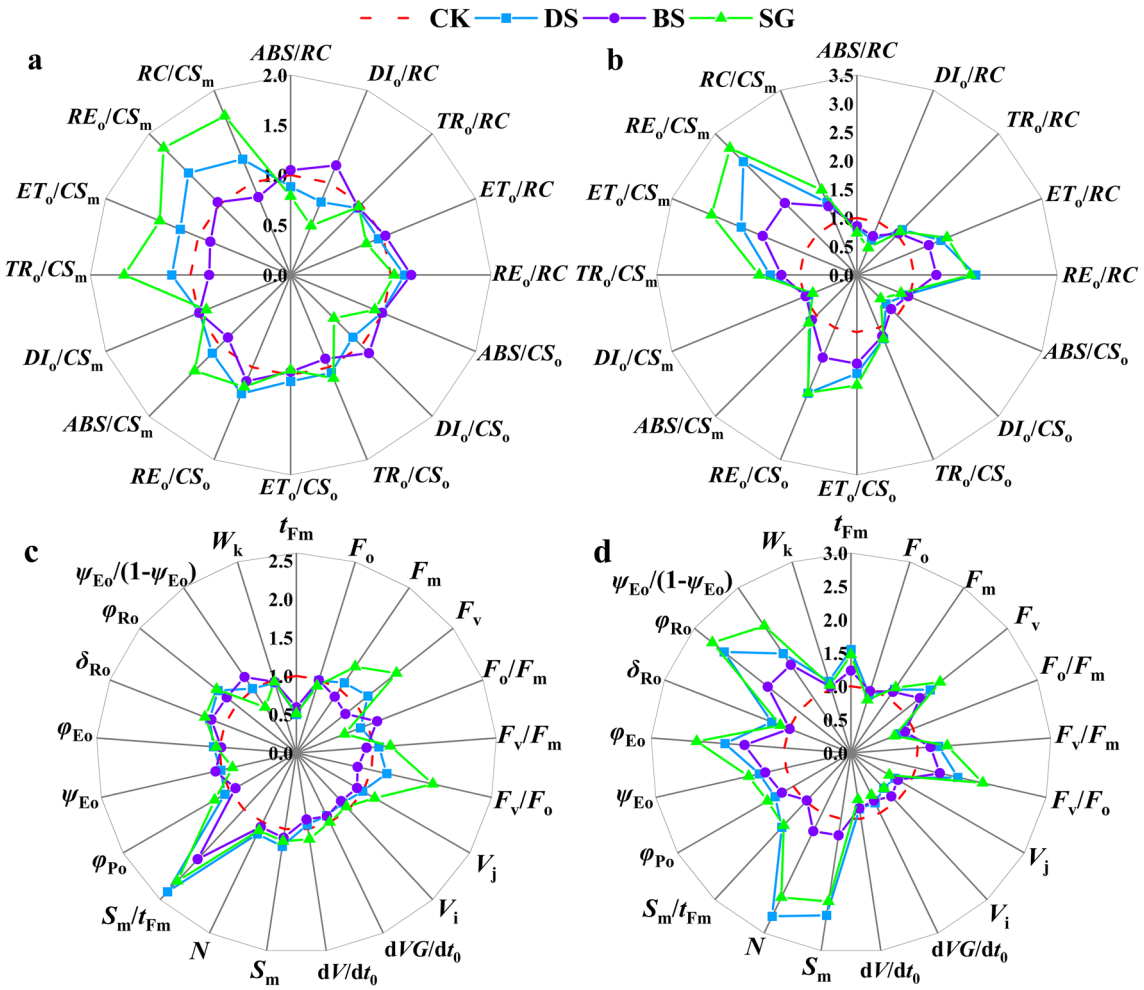

Fig. 6 The effects of different treatments on the JIP-test parameters of cucumber seedling leaves after low-temperature stress (day (10 ± 1) °C/14 h, night (6 ± 1) °C/10 h). **a** and **b** The specific activity of the leaf photosynthetic apparatus. **c** and **d** The performance parameter. **a** and **c** Low temperature for 24 h, **b** and **d** Low temperature for 48 h. The value is the mean ± SD ($n = 3$)

significantly increased $\Delta I/I_o$ by 8.10% and 16.98% after 24 h and 48 h of low temperature compared to CK, respectively. Compared with the DS, BS treatment significantly attenuated the SNP-induced $\Delta I/I_o$ elevation. BS treatment significantly reduced $\Delta I/I_o$ by 21.59% and 21.45%, respectively, after 24 h and 48 h of low temperature compared with that in DS. In addition, the SG treatment significantly increased $\Delta I/I_o$ by 13.45% and 20.19% after 24 and 48 h of low temperature compared to CK. The SG treatment has the largest $\Delta I/I_o$ value compared to the other treatments.

Discussion

Cell membrane damage is a rapid stress response caused by low temperature, and this change can be characterized by EL (Marangoni et al. 1996). In our study, compared with the cucumber seedling leaves treated with distilled water (CK), the cucumber seedling treated with SNP (DS) and SNP + GSH (SG) showed significantly decreased EL after 24 h of low temperature, which indicated that the DS and SG treatment could effectively alleviate cell damage caused by low temperature. With the extension of the low-temperature time to 48 h, the EL of the SG treatment was significantly lower than that of the DS treatment, indicating that the SG treatment had the best effect on alleviating membrane damage at prolonged low temperature. In addition, the cucumber seedling treated with BSO + SNP (BS) showed significantly increased EL after 48 h of low temperature, indicating that the protective effect of SNP on membrane damage could be reversed by BSO. (Fig. 3).

Oxidative stress and physiological water stress induced by low temperature can be alleviated by the application of NO and GSH. Under low temperatures, the impaired enzyme activities related to physiological metabolism, lead to physiological water shortage. The typical response

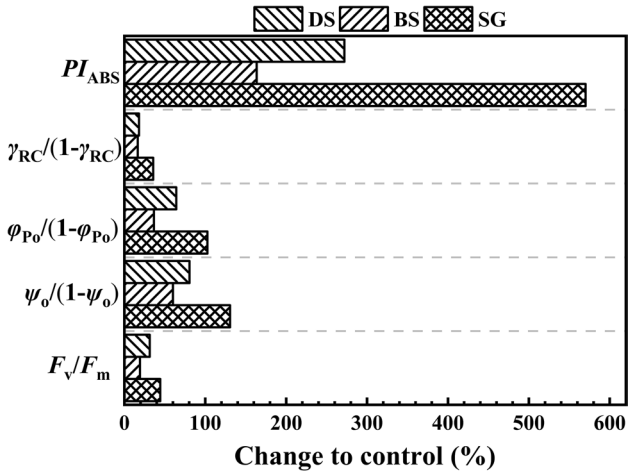

Fig. 7 Effect of different treatments on PI_{ABS} and its related response components after 48 h of low-temperature stress. The density of the effective photosystem ($\gamma_{RC}/(1-\gamma_{RC})$, the efficiency of primary photochemistry (capture) ($\varphi_{Po}/(1-\varphi_{Po})$, the efficiency of conversion of excitation energy into electron transport ($\psi_o/(1-\psi_o)$, and the maximum photochemical quantum yield (F_v/F_m). Horizontal bars indicate the response in dark-cooled plants relative to control plants

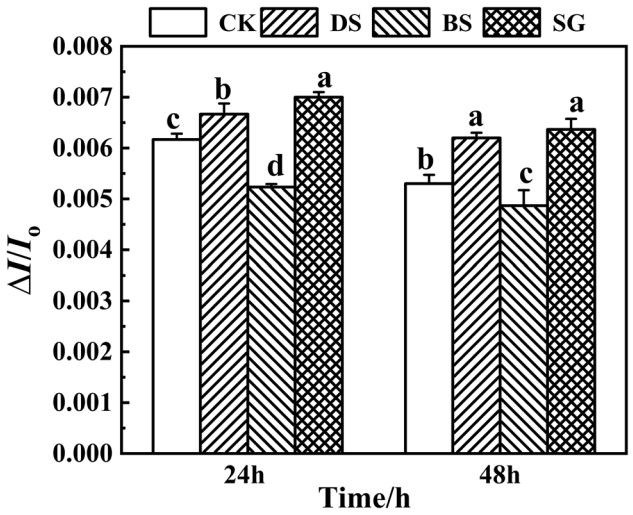

Fig. 8 Effects of different treatments on the $\Delta I/I_o$ of cucumber seedling leaves after low-temperature stress. Different letters indicate statistically significant differences ($P < 0.05$)

of organisms to water deficit is an osmotic adjustment. The low temperature-induced oxidative stress could destroy the balance between ROS production and removal, leading to a large amount of ROS accumulation (Ruelland et al. 2009). The accumulation of large amounts of osmoregulatory substances and the enhancement of the antioxidant system (AsA-GSH cycle) are crucial to resisting abiotic stress. The increase of proline, a representative osmotic regulator, has a positive influence on the cold resistance in plants. For example, relieving physiological dehydration and plasma membrane stability would form hydrophilic colloids to protect protein molecules, which scavenge the ROS and store energy under abiotic stress (Ben Rejeb et al. 2014). Previous studies have shown a close relationship between NO, lipid metabolism, and Pro accumulation during low-temperature acclimation (He and He 2018). Exogenous NO could increase the accumulation of Pro in bamboo shoots (Wang et al. 2017). Exogenous NO at low temperatures can achieve mitigation of cellular damage through the accumulation of osmoregulatory substances and increased activity of antioxidant enzymes (AsA-GSH cycle) (Wu et al. 2020). In addition, our previous study found that both SNP and GSH, applied alone or in combination, increased APX activity in the AsA-GSH cycle (Yang et al. 2020). In the current study, compared with DS, the SG treatment significantly reduced the accumulation of $O_2^{-\bullet}$ and H_2O_2, and increased the Pro content, GR, MDHAR, DHAR, GPX, and GST activities after 24 h of low temperature. With the extension of low-temperature time, the ameliorative effect of SG treatment became more and more prominent (Figs. 2 and 4).

The synergistic effect of NO and GSH ameliorates the decrease in PSII activity caused by low temperature and promotes the electron flow between PSII and PSI. Compared with F_v/F_m, PI_{ABS} can more effectively reflect the actual activity of PSII. The parameters of $\varphi_{Po}/(1-\varphi_{Po})$ and $\psi_o/(1-\psi_o)$ are important relevant response components of PI_{ABS} (Strauss et al. 2006). The values of PI_{ABS}, $\varphi_{Po}/(1-\varphi_{Po})$, and $\psi_o/(1-\psi_o)$ were greater than 0 for DS treatment compared with CK at 48 h of low temperature (Fig. 7), implying that the effect of NO on PSII activity restoration after adversity was achieved mainly by increasing the efficiency of reaction centers, light energy uptake efficiency and electron acceptor acceptance efficiency. It was consistent with previous studies that plants treated with NO would enhance leaf photosynthesis by increasing the electron transport of PSII (Vladkova et al. 2011), under abiotic stresses such as drought stress (Santisree et al. 2015), and Cr(VI) toxicity (Alamri et al. 2020). Interestingly, we found that the PI_{ABS}, $\varphi_{Po}/(1-\varphi_{Po})$, and $\psi_o/(1-\psi_o)$ of the SG treatment are larger than those of the DS treatment (Fig. 7), indicating that the addition of GSH (SNP + GSH treatment) exerted a synergistic effect in SNP action to restore plant photosynthetic capacity. It was worth mentioning that access to the changes on the donor and acceptor sites of PSII was an important aspect in the analysis of the effect of low temperature on PSII. Firstly, we analyzed the changes in the donor site of PSII. Some studies have shown that the oxygen-evolving complex of plant leaves is damaged to different degrees exposed to abiotic stresses, such as high temperature (Yanhui et al. 2020), resulting in elevated K-step. In this paper, under the short duration low-temperature stress (24 h), DS and SG treatments had

higher K-step (Fig. 5a and b), and the opposite phenomenon occurred with the extension of the low-temperature time to 48 h. Based on the different phenomena mentioned above, we speculated that with the prolongation of low-temperature time, there was no accumulation of ROS, and the limitation of electron flow on the oxidation site of PSII was no longer the main factor affecting photosynthesis. Each site redox state has the potential to affect the overall electron transfer efficiency during electron flow from the oxygen-evolving complex to the end of the PSI (Sánchez-Moreiras and Reigosa 2018). Next, there was an analysis of the changes in the PSII receptor site. The parameter of φ_{Eo} reflects the probability that the light energy absorbed by the reaction center can transfer electrons to other electron acceptors in the electron transport chain over Q_A. The parameter of S_m reflects the energy required to make Q_A completely reduced, which is the size of the PQ pool on the receptor site of the PSII reaction center. The more electrons enter the electron transport chain from Q_A^-, the longer it takes to reach F_m, and the larger the value of S_m. Low-temperature stress leads to a decrease in φ_{Eo} and S_m (Strasserf et al. 1995; Heerden et al. 2003). In our research, with the extension of the low-temperature time to 48 h, DS, BS, and SG treatments were greater than CK (especially DS and SG treatments) (Fig. 6d), implying that all treatment groups (DS, BS, and SG) could effectively maintain φ_{Eo} and S_m which was a capacity of the electron acceptor pool on the site of PSII receptors in cucumber leaves, where the spraying of NO, NO + GSH was more effective to protect the PSII receptor site. In addition, the flow of the photosynthetic electron transport chain is also a crucial aspect. After 48 h of low temperature, DS treatment significantly reduced V_J (Fig. 4c) and increased photosynthetic mechanism ratio active parameters TR_o/CS_m, ET_o/CS_m, RE_o/CS_m compared to CK (Fig. 6a and b). And this phenomenon suggested that NO promoted the flow of electrons from PSII to PSI, which was consistent with the previous study that NO could improve the photosynthetic capacity under adversity (Vladkova et al. 2011). The smaller V_J values of the SG treatment with larger values of the photosynthetic machinery than the activity parameters (TR_o/CS_m, ET_o/CS_m, RE_o/CS_m) compared to SNP alone implying that cooperative actions of NO and GSH were more conducive to electron flow.

In comparison with PSII, PSI did not have a fast turnover mechanism similar to the D1 protein leading to lower activity (Zhang and Scheller 2004). The large amounts of electrons flowing from PSII to PSI would combine with oxygen molecules at PSI leading to the accumulation of ROS, which further inhibited the recovery of PSI activity by disrupting the membrane structure causing the weakening of electron transfer efficiency (Zhang and Scheller 2004; Asada 2006). Therefore, the effective removal of ROS is very important for the functional maintenance of PSI. MR is widely used in leaf PSI activity studies, and $\Delta I/I_o$ is a critical parameter for measuring PSI activity (Strasser et al. 2010). After 24 h of exposure to low temperature, DS treatment significantly increased the amount of Pro (Fig. 3) and the activity of enzymes (GR, MDHAR, DHAR, GPX, and GST) (Fig. 4), and $\Delta I/I_o$ compared with CK (Fig. 8) (Ahanger et al. 2019). Our previous study found that NO could promote the increase of osmotic substances and the activity of antioxidant enzymes related to the AsA-GSH cycle to achieve effective protection from ROS at PSI sites (Yang et al. 2020). Also, RC was negatively correlated with Pro, antioxidant enzymes (GR, MDHAR, DHAR, GPX and GST), and $\Delta I/I_o$ exactly to further validate the above findings (Fig. S1).

When plants are deficient in GSH such as GSH mutants *rax1-1*, which is compromised in the maintenance of cellular redox environment and many other aspects (Dubreuil-Maurizi et al. 2011). Arabidopsis mutants deficient in GSH biosynthesis and plants under BSO treatment show inhibited root growth by modulating total ubiquitination of proteins and increasing the stability of Aux/IAA proteins inhibiting the expression of classical auxin-responsive genes (Pasternak et al. 2020). This indicates that GSH is a significant enhancer of auxin signaling under stress conditions. The BSO is an inhibitor of γ-ECS (EC 6.3.2.2), which is a key enzyme for GSH synthesis (Drew and Miners 1984). In addition, the effect of the NO was partially inhibited by BSO in this experiment. Compared to DS treatment at low temperature for 48 h, the BS treatment significantly reduced the activities of antioxidant enzymes (GR, MDHAR, DHAR, GPX, GST) of AsA-GSH cycles and the Pro content and increased the electrolyte permeability (Figs. 3 and 4), indicating that BSO attenuated the effect of NO on ROS mitigation. For photosynthesis, BS treatment increased V_J, ΔV_I (Fig. 5), and decreased PI_{ABS} and $\Delta I/I_o$ (Fig. 8) compared to DS at low temperature for 48 h, showing that BSO induced the shutdown of PSII (active reaction center (P_{680}), electron transport activity from Q_A to Q_B and Q_B to PSI (P_{680}), and the weakening of PSI activity. The response component analysis of PI_{ABS} revealed that BSO attenuated the restoration effect of NO on low-temperature photosynthesis, probably through the reduction of ($\varphi_{(Po)}/(1-\varphi_{(Po)})$ and ($\psi_o/(1-\psi_o)$) value (Fig. 7), specifically in the reduction of the specific activity and performance parameters of leaf photosynthetic machinery (Fig. 6). BSO severely inhibited the mitigating effect of SNP under cold stress, whereas SG treatment had an additive effect, indicating that GSH is indispensable in NO-induced alleviation of cold stress. GSH may play a role downstream of NO, and the combined application of NO and GSH was more effective in improving the cold tolerance of cucumber seedlings.

NO also regulates GSH concentration in several ways. NO may react with GSH to form GSNO, which is the main

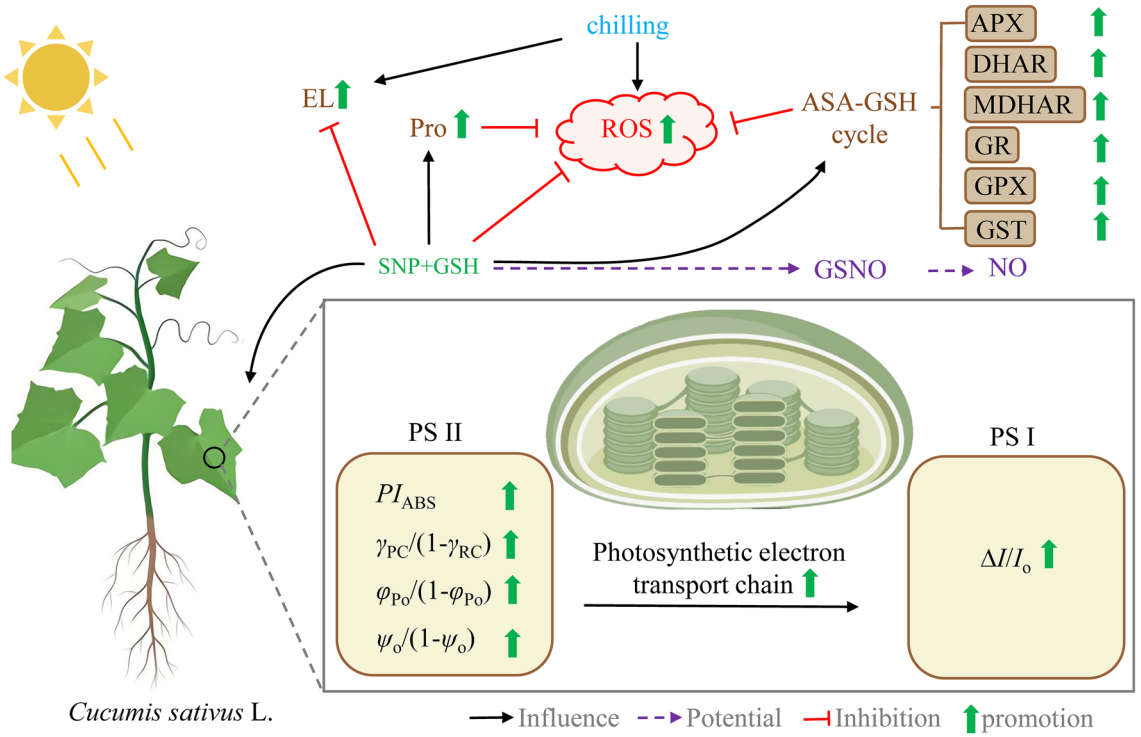

Fig. 9 Model representing the potential mechanism of exogenous NO synergistic with GSH to alleviate low-temperature stress in cucumber seedlings (day (10 ± 1) °C/14 h, night (6 ± 1) °C/10 h). Low-temperature stress causes oxidative stress in plants through the production of reactive oxygen species. On the one hand, the application of SNP synergistic with GSH can alleviate low temperature-induced oxidative stress by increasing Pro content, decreasing EL, and enhancing AsA-GSH cycle system enzyme activities (DHAR, MDHAR, GR, GPX, and GST activities). On the other hand, the combined application of SNP and GSH promoted the PSII activity (PI_{ABS}), PSI activity ($\Delta I/I_o$) and electron flow between the electron transport chains to alleviate the low temperature-induced photoinhibition and thereby protect the normal growth of cucumber seedlings. SNP, sodium nitroprusside; GSH, reduced glutathione; GSNO, *S*-nitrosoglutathione; NO, nitric oxide; ROS, reactive oxygen species; EL, electrolyte leakage; Pro, proline; AsA-GSH, ascorbate–glutathione cycle; DHAR, dehydroascorbate reductase; MDHAR, monodehydroascorbate reductase; GR, glutathione reductase; GPX, glutathione peroxidase; GST, glutathione-*S*-transferase; PSII, photosystem II; PSI, photosystem I; PI_{ABS}, performance index on absorption basis; $\Delta I/I_o$, the measure of maximum PSI activity (I_o is the maximum value of 820 nm light absorption and I_m is the minimum value of 820 nm light absorption); ($\gamma_{RC}/(1-\gamma_{RC})$, the density of the effective photosystem; ($\varphi_{Po}/(1-\varphi_{Po})$, the efficiency of primary photochemistry (capture); ($\psi_o/(1-\psi_o)$, the efficiency of conversion of excitation energy into electron transport

source of NO reservoir and *S*-nitrosylation. GSNO can be catabolized by GSNO reductase (GSNOR) to GSSG, which in turn is reduced to GSH by GR. GSNOR may also be inhibited by *S*-nitrosylation and NO-activated GR (Broniowska et al. 2013). One of the reasons why SNP applications work better with GSH is because plants can regulate free NO concentrations more effectively through GSNO, in addition to acting as a reservoir. In conclusion, we showed that NO collaborates with GSH to improve the cold resistance of cucumber seedlings. SG treatment could protect membrane integrity (EL reduction), increase PSII activity (ABS, TR, and electron transport efficiency), promote electron transport chain including PSII flow to PSI terminus, increase PSI activity, and mitigate the adverse effects of low temperature on photosynthesis through cellular osmoregulation and ROS scavenging system (Fig. 9). We speculated that the reason for it is that both NO and GSH could improve the above-mentioned cold resistance at low temperatures (Fancy et al. 2017; Hasanuzzaman et al. 2017). Moreover, the half-life of NO in vivo is very short in plants (Begara-Morales et al. 2018). NO may exert biological activity through *S*-nitrosylation (lipophilic NO and GSH form GSNO) (Lindermayr 2017). Potential GSNO as a long-distance signal molecule extends the function of NO on a Spatio-temporal basis (Begara-Morales et al. 2018). In addition, the application of NO upregulated endogenous GSH (Zhang et al. 2019), which might also be one of the possible reasons for the superior effect of the combined treatment.

Supplementary Information The online version contains supplementary material available at https://doi.org/10.1007/s00344-023-10936-x.

Acknowledgements We are grateful to Golam Jalal Ahammed for helping us improve our manuscript.

Author Contributions This work was carried out in collaboration with all the authors. ZY and JC conceived and designed the experiment. ZY and XW conducted the experiments, data analysis, and wrote the original draft. JC, HL, HC, and PW: reviewed and edited the manuscript. All authors have contributed to seeing and approving the final manuscript.

Funding We are grateful to the National Natural Science Foundation of China (No.31560571) for providing financial support to our research.

Declarations

Conflict of interest The authors declare that they have no conflict of interest.

References

Adamski JM, Peters JA, Danieloski R, Bacarin MA (2011) Excess iron-induced changes in the photosynthetic characteristics of sweet potato. J Plant Physiol 168(17):2056–2062. https://doi.org/10.1016/j.jplph.2011.06.003

Ahanger MA, Aziz U, Alsahli AA, Alyemeni MN, Ahmad P (2019) Influence of exogenous salicylic acid and nitric oxide on growth, photosynthesis, and ascorbate-glutathione cycle in salt stressed *Vigna angularis*. Biomolecules 10(1):16. https://doi.org/10.3390/biom10010042

Alamri S, Ali HM, Khan MIR, Singh VP, Siddiqui MH (2020) Exogenous nitric oxide requires endogenous hydrogen sulfide to induce the resilience through sulfur assimilation in tomato seedlings under hexavalent chromium toxicity. Plant Physiol Biochem 155:20–34. https://doi.org/10.1016/j.plaphy.2020.07.003

Asada K (2006) Production and scavenging of reactive oxygen species in chloroplasts and their functions. Plant Physiol 141(2):391–396. https://doi.org/10.1104/pp.106.082040

Begara-Morales JC, Chaki M, Valderrama R, Sanchez-Calvo B, Mata-Perez C, Padilla MN, Corpas FJ, Barroso JB (2018) Nitric oxide buffering and conditional nitric oxide release in stress response. J Exp Bot 69(14):3425–3438. https://doi.org/10.1093/jxb/ery072

Ben Rejeb K, Abdelly C, Savoure A (2014) How reactive oxygen species and proline face stress together. Plant Physiol Biochem 80:278–284. https://doi.org/10.1016/j.plaphy.2014.04.007

Booth J, Boyland E, Sims P (1961) An enzyme from rat liver catalysing conjugations with glutathione. Biochem J 79(3):516–524. https://doi.org/10.1042/bj0790516

Broniowska KA, Diers AR (1830) Hogg N (2013) *S*-nitrosoglutathione. Biochim Biophys Acta 5:3173–3181. https://doi.org/10.1016/j.bbagen.2013.02.004

Cabrera RM, Saltveit ME, Owens K (1992) Cucumber cultivars differ in their response to chilling temperatures. J Am Soc Hortic Sci 117(5):802–807. https://doi.org/10.21273/jashs.117.5.802

Dawood MG, Sadak MS, Bakry BA, Kheder HH (2020) Effect of glutathione and/or selenium levels on growth, yield, and some biochemical constituents of some wheat cultivars grown under sandy soil conditions. Bull Natl Res Centre 44:158. https://doi.org/10.1186/s42269-020-00410-z

Ding Y, Shi Y, Yang S (2019) Advances and challenges in uncovering cold tolerance regulatory mechanisms in plants. New Phytol 222(4):1690–1704. https://doi.org/10.1111/nph.15696

Drew R, Miners JO (1984) The effects of buthionine sulphoximine (BSO) on glutathione depletion and xenobiotic biotransformation. Biochem Pharmacol 33:2989–2994. https://doi.org/10.1016/0006-2952(84)90598-7

Dubreuil-Maurizi C, Vitecek J, Marty L, Branciard L, Frettinger P, Wendehenne D, Meyer AJ, Mauch F, Poinssot B (2011) Glutathione deficiency of the *Arabidopsis* mutant *pad2-1* affects oxidative stress-related events, defense gene expression, and the hypersensitive response. Plant Physiol 157(4):2000–2012. https://doi.org/10.1104/pp.111.182667

Elkhatib H, Gabr SM, Elazomy AA (2021) Salt stress relief and growth-promoting effect of sweet pepper plants (*Capsicum annuum* L.) by glutathione, selenium, and humic acid application. Alexandria Sci Exch J 42:583–608. https://doi.org/10.21608/asejaiqjsae.2021.183461

Fancy NN, Bahlmann AK, Loake GJ (2017) Nitric oxide function in plant abiotic stress. Plant, Cell Environ 40(4):462–472. https://doi.org/10.1111/pce.12707

Goodarzi A, Namdjoyan S, Soorki AA (2020) Effects of exogenous melatonin and glutathione on zinc toxicity in safflower (*Carthamus tinctorius* L) seedlings. Ecotoxicol Environ Saf 201:110853. https://doi.org/10.1016/j.ecoenv.2020.110853

Gupta DK, Palma JM, Corpas FJ (2015) Modulation of the ascorbate–glutathione cycle antioxidant capacity by posttranslational modifications mediated by nitric oxide in abiotic stress situations. React Oxyg Species Oxid Damage Plants under Stress. https://doi.org/10.1007/978-3-319-20421-5

Hasanuzzaman M, Nahar K, Anee TI, Fujita M (2017) Glutathione in plants: biosynthesis and physiological role in environmental stress tolerance. Physiol Mole Biol Plants 23(2):249–268. https://doi.org/10.1007/s12298-017-0422-2

He H, He LF (2018) Regulation of gaseous signaling molecules on proline metabolism in plants. Plant Cell Rep 37(3):387–392. https://doi.org/10.1007/s00299-017-2239-4

Hu LL, Li YT, Wu Y, Lv J, Dawuda MM, Tang ZQ, Liao WB, Calderon-Urrea A, Xie JM, Yu JH (2019) Nitric oxide is involved in the regulation of the ascorbate-glutathione cycle induced by the appropriate ammonium: nitrate to mitigate low light stress in *Brassica pekinensis*. Plants-Basel 8(11):14. https://doi.org/10.3390/plants8110489

Jahan A, Iqbal M, Shafiq F, Malik A, Javed MT (2021) Influence of foliar glutathione and putrescine on metabolism and mineral status of genetically diverse rapeseed cultivars under hexavalent chromium stress. Environ Sci Pollut Res 28(33):45353–45363. https://doi.org/10.1007/s11356-021-13702-2

Khoshbakht D, Asghari MR, Haghighi M (2018) Effects of foliar applications of nitric oxide and spermidine on chlorophyll fluorescence, photosynthesis and antioxidant enzyme activities of citrus seedlings under salinity stress. Photosynthetica 56(4):1313–1325. https://doi.org/10.1007/s11099-018-0839-z

Li HS (2000) Principles and techniques of plant physiological and biochemical experiment. Higher Education Press, Beijing.

Lindermayr C (2017) Crosstalk between reactive oxygen species and nitric oxide in plants: key role of *S*-nitrosoglutathione reductase. Free Radical Biol Med 122:110–115. https://doi.org/10.1016/j.freeradbiomed.2017.11.027

Ma CX, Liu H, Chen GC, Zhao Q, Guo HY, Minocha R, Long S, Tang YZ, Saad EM, DeLaTorreRoche R, White JC, Xing BS, Dhankher OP (2020) Dual roles of glutathione in silver nanoparticle detoxification and enhancement of nitrogen assimilation in soybean (*Glycine max* L. [Merrill]). Environ-Sci Nano 7(7):1954–1966. https://doi.org/10.1039/d0en00147c

Marangoni AG, Palma T, Stanley DW (1996) Membrane effects in postharvest physiology. Postharvest Biol Technol 7(3):193–217. https://doi.org/10.1016/0925-5214(95)00042-9

Miller G, Suzuki N, Rizhsky L, Hegie A, Koussevitzky S, Mittler R (2007) Double mutants deficient in cytosolic and thylakoid ascorbate peroxidase reveal a complex mode of interaction between reactive oxygen species, plant development, and response to

abiotic stresses. Plant Physiol 144(4):1777–1785. https://doi.org/10.1104/pp.107.101436
Mishra AN (2018) Chlorophyll fluorescence: a practical approach to study ecophysiology of green plants. Adv Plant Ecophysiol Tech. https://doi.org/10.1007/978-3-319-93233-0_5
Mostofa MG, Seraj ZI, Fujita M (2015) Interactive effects of nitric oxide and glutathione in mitigating copper toxicity of rice (*Oryza sativa* L.) seedlings. Plant Signal Behavior 10(3):1–4. https://doi.org/10.4161/15592324.2014.991570
Nam HI, Shahzad Z, Dorone Y, Clowez S, Zhao K, Bouain N, Cho H, Rhee SY, Rouached H (2021) Interdependent iron and phosphorus availability controls photosynthesis through retrograde signaling. Nat Commun. https://doi.org/10.1101/2021.02.11.430802
Pasternak T, Palme K, Paponov IA (2020) Glutathione enhances auxin sensitivity in *Arabidopsis* roots. Biomolecules 10(11):1550–11574. https://doi.org/10.3390/biom10111550
Rai KK, Rai N, Rai SP (2018) Salicylic acid and nitric oxide alleviate high temperature induced oxidative damage in *Lablab purpureus* L plants by regulating bio-physical processes and DNA methylation. Plant Physiol Biochem 128:72–88. https://doi.org/10.1016/j.plaphy.2018.04.023
Rehman HU, Alharby HF, Bamagoos AA, Abdelhamid MT, Rady MM (2021) Sequenced application of glutathione as an antioxidant with an organic biostimulant improves physiological and metabolic adaptation to salinity in wheat. Plant Physiol Biochem 158:43–52
Rigui AP, Carvalho V, Wendt Dos Santos AL, Morvan-Bertrand A, Prud'homme MP, Machado de Carvalho MA, Gaspar M (2019) Fructan and antioxidant metabolisms in plants of *Lolium perenne* under drought are modulated by exogenous nitric oxide. Plant Physiol Biochem 145:205–215. https://doi.org/10.1016/j.plaphy.2019.10.029
Ruelland E, Vaultier MN, Zachowski A, Hurry V (2009) Cold signalling and cold acclimation in plants. Adv Bot Res 49:35–150. https://doi.org/10.1016/s0065-2296(08)00602-2
Sánchez-Moreiras AM, Reigosa MJ (2018) Advances in plant ecophysiology techniques. Springer International Publishing, Cham
Santisree P, Bhatnagar-Mathur P, Sharma KK (2015) NO to drought-multifunctional role of nitric oxide in plant drought: do we have all the answers? Plant Sci 239:44–55. https://doi.org/10.1016/j.plantsci.2015.07.012
Silveira NM, Frungillo L, Marcos FC, Pelegrino MT, Miranda MT, Seabra AB, Salgado I, Machado EC, Ribeiro RV (2016) Exogenous nitric oxide improves sugarcane growth and photosynthesis under water deficit. Planta 244(1):181–190. https://doi.org/10.1007/s00425-016-2501-y
Song L, Yue L, Zhao H, Hou M (2013) Protection effect of nitric oxide on photosynthesis in rice under heat stress. Acta Physiol Plant 35(12):3323–3333. https://doi.org/10.1007/s11738-013-1365-z
Strasser RJ, Tsimilli-Michael M, Qiang S, Goltsev V (2010) Simultaneous in vivo recording of prompt and delayed fluorescence and 820-nm reflection changes during drying and after rehydration of the resurrection plant *Haberlea rhodopensis*. Biochem Biophys Acta 1797(6–7):1313–1326. https://doi.org/10.1016/j.bbabio.2010.03.008
Strasserf RJ, Srivastava A (1995) Polyphasic chlorophyll a fluorescence transient in plants and cyanobacteria. Photochem Photobiol 61(1):32–42. https://doi.org/10.1111/j.1751-1097.1995.tb09240.x
Strauss AJ, Kruger GHJ, Strasser RJ, Van Heerden PDR (2006) Ranking of dark chilling tolerance in soybean genotypes probed by the chlorophyll a fluorescence transient O-J-I-P. Environ Exp Bot 56(2):147–157. https://doi.org/10.1016/j.envexpbot.2005.01.011
Sun C, Zhang Y, Liu L, Liu X, Li B, Jin C, Lin X (2021) Molecular functions of nitric oxide and its potential applications in horticultural crops. Horticult Res 8(1):71. https://doi.org/10.1038/s41438-021-00500-7
Tewari RK, Horemans N, Watanabe M (2021) Evidence for a role of nitric oxide in iron homeostasis in plants. J Exp Bot 72(4):990–1006. https://doi.org/10.1093/jxb/eraa484
Thordal-Christensen H, Zhang Z, Wei Y, Collinge DB (1997) Subcellular localization of H2O2 in plants H2O2 accumulation in papillae and hypersensitive response during the barley—powdery mildew interaction. J Plant 11(6):1187–1194. https://doi.org/10.1046/j.1365-313X.1997.11061187.x
Van Heerden PD, Tsimilli-Michael M, Krüger GH, Strasser RJ (2003) Dark chilling effects on soybean genotypes during vegetative development: parallel studies of CO_2 assimilation, chlorophyll a fluorescence kinetics O-J-I-P and nitrogen fixation. Physiol Plant 117:476–491. https://doi.org/10.1034/j.1399-3054.2003.00056.x
Vladkova R, Dobrikova AG, Singh R, Misra AN, Apostolova E (2011) Photoelectron transport ability of chloroplast thylakoid membranes treated with NO donor SNP: changes in flash oxygen evolution and chlorophyll fluorescence. Nitric Oxide 24(2):84–90. https://doi.org/10.1016/j.niox.2010.12.003
Wang D, Li L, Xu YQ, Limwachiranon J, Li D, Ban ZJ, Luo ZS (2017) Effect of exogenous nitro oxide on chilling tolerance, polyamine, proline, and gamma-aminobutyric acid in bamboo shoots (Phyllostachys praecox f. prevernalis). J Agric Food Chem 65(28):5607–5613. https://doi.org/10.1021/acs.jafc.7b02091
Waszczak C, Carmody M, Kangasjarvi J (2018) Reactive oxygen species in plant signaling. Annu Rev Plant Biol 69:209–236. https://doi.org/10.1146/annurev-arplant-042817-040322
Wojcik M, Tukiendorf A (2011) Glutathione in adaptation of *Arabidopsis* thaliana to cadmium stress. Biol Plant 55(1):125–132. https://doi.org/10.1007/s10535-011-0017-7
Wu P, Xiao C, Cui J, Hao B, Zhang W, Yang Z, Ahammed GJ, Liu H, Cui H (2020) Nitric oxide and its interaction with hydrogen peroxide enhance plant tolerance to low temperatures by improving the efficiency of the calvin cycle and the ascorbate–glutathione cycle in cucumber seedlings. J Plant Growth Regul. https://doi.org/10.1007/s00344-020-10242-w
Yang ZF, Wang XY, Cui JX, Liu HY, Zhang WB, Wu P (2020) Synergistic effect of exogenous NO and GSH under chilling stress to improve cold tolerance of cucumber seedlings. Plant Physiol J. https://doi.org/10.13592/j.cnki.ppj.2020.0036
Yanhui C, Hongrui W, Beining Z, Shixing G, Zihan W, Yue W, Huihui Z, Guangyu S (2020) Elevated air temperature damage to photosynthetic apparatus alleviated by enhanced cyclic electron flow around photosystem I in tobacco leaves. Ecotoxicol Environ Saf 204:111136. https://doi.org/10.1016/j.ecoenv.2020.111136
Yun BW, Skelly MJ, Yin M, Yu M, Mun BG, Lee SU, Hussain A, Spoel SH, Loake GJ (2016) Nitric oxide and *S*-nitrosoglutathione function additively during plant immunity. New Phytol 211(2):516–526. https://doi.org/10.1111/nph.13903
Zandalinas SI, Balfagon D, Arbona V, Gomez-Cadenas A (2018) Regulation of citrus responses to the combined action of drought and high temperatures depends on the severity of water deprivation. Physiol Plant 162(4):427–438. https://doi.org/10.1111/ppl.12643
Zeng F, Mallhi ZI, Khan N, Rizwan M, Ali S, Ahmad A, Hussain A, Alsahli AA, Alyemeni MN (2021) Combined citric acid and glutathione augments lead (Pb) stress tolerance and phytoremediation of castorbean through antioxidant machinery and Pb uptake. Sustainability. https://doi.org/10.3390/su13074073
Zhang SP, Scheller HV (2004) Photoinhibition of photosystem I at chilling temperature and subsequent recovery in *Arabidopsis thaliana*. Plant Cell Physiol 45(11):1595–1602. https://doi.org/10.1093/pcp/pch180
Zhang PP, Li SS, Guo ZF, Lu SY (2019) Nitric oxide regulates glutathione synthesis and cold tolerance in forage legumes. Environ Exp Bot 167:8. https://doi.org/10.1016/j.envexpbot.2019.103851
Zhou Y, Huang L, Zhang Y, Shi K, Yu J, Nogues S (2007) Chill-induced decrease in capacity of RuBP carboxylation and

associated H_2O_2 accumulation in cucumber leaves are alleviated by grafting onto figleaf gourd. Ann Bot 100(4):839–848. https://doi.org/10.1093/aob/mcm181

Zhou Y, Diao M, Cui JX, Chen XJ, Wen ZL, Zhang JW, Liu HY (2018) Exogenous GSH protects tomatoes against salt stress by modulating photosystem II efficiency, absorbed light allocation and H_2O_2-scavenging system in chloroplasts. J Integr Agric 17(10):2257–2272. https://doi.org/10.1016/s2095-3119(18)62068-4